Military Technical College
Kobry El-Kobbah,
Cairo, Egypt.

17th International Conference
on Applied Mechanics and
Mechanical Engineering.

HEAT TRANSFER ENHANCEMENT FROM ELECTRONIC MODULE IN A HORIZONTAL CHANNEL USING A CURVED DEFLECTOR

A.S. Rosas[1,*], R.K. Khalil[1], A.A. Abdel-Aziz[1] and K.M. El-Shzaly[1]

ABSTRACT

This work investigated experimentally the heat transfer and pressure drop from an electronic module of two heat sources inserted in rectangular horizontal channel, having curved deflector to direct the flow. The experiments were carried out to investigate the deflector dimensionless radius (R_r) and both horizontal and vertical dimensionless distances (R_x, R_y) within a range of Reynolds number from 5223 to 11338. The results show that larger deflector with small vertical distance enhances the heat transfer for upstream and downstream heat sources while the horizontal distance has a contrast effect on the heat sources. Correlations are obtained for the average Nusselt number of both upstream and downstream heat sources utilizing the present measurements within the investigated range of geometrical parameters and Reynolds number.

KEYWORDS

Electronic chip, Cooling, Curved deflector, turbulent

---

[1] Mechanical Engineering Department, Faculty of Engineering Shoubra, Benha University, 108 Shoubra Street, Shoubra, Cairo 11689, Egypt.

* Corresponding author: Tel: 00201001757488, Email: Ahmedresas@gmail.com.

NOMENCLATURE

Symbols:

A	surface area, m^2
B	heat source height, m
D_h	hydraulic diameter, D_h=0.133, m
h	heat transfer coefficient, W/m^2. K
H	channel height, m
K	thermal conductivity of the fluid, w/m.k
L	heat source length, m
ℓ	length across test section, m
P	pressure, Pa
q	heat transfer rate, W
q"	Heat flux, W/m^2
R	resistance, Ω
r	deflector radius, mm
R_r	dimensionless radius of the deflector, R/L
R_x	dimensionless position of the deflector in X-coordinate , X/L
R_y	dimensionless position of the deflector in Y-coordinate, y/L
S	the separation distance, m
T	temperature, K
U_{ave}	average flow velocity, m /s
V	voltage ,V
X	horizontal distance from deflector tip to upstream source, mm
y	vertical distance from deflector lower tip to lower duct wall , mm

Subscripts

a	Inlet fluid temperature
Basic	basic module without deflector
con	heat lost by conduction
def	deflector
in	input
L	based on the heat source length
m	mean temperature of the heat source
net	net heat transferred to fluid
rad	heat lost by radiation
Or	orifice

Greek letters

Δ	difference value
ρ	density , Kg/m3
μ	Dynamic viscosity, Kg/m.s
	Dimensionless terms
f	Fanning friction factor, $f = \frac{2\Delta P * D_h/l}{\rho {U_m}^2}$
Nu_L	average Nusselt number, Nu = h* L /K

Re_L Reynolds number , $Re_L = \frac{\rho U_m L}{\mu}$

Nu_L average Nusselt number, Nu = h* L /K

INTRODUCTION

Air-cooling technology has gained a top ranking among electronic cooling techniques for its performance, reliability, reasonable cost, space occupation, and low power consumption [1, 2]. The drawback of air cooling is that the heat fluxes that can be achieved today using air-cooling were achievable in 1980s only by means of liquid cooling[1]. Over limit temperatures lead to excessive strain and cause physical breakdown. In order to avoid over limit temperature, two approaches can be followed. The first one is suitable for moderate heat removal applications where the flow rate of the coolant can be increased. This solution is limited for the generated noise and the coolant pumping power [3].The second approach involves modification of the channel topology while keeping fixed the coolant flow rate.

Previous studies have demonstrated that the heat transfer along a horizontal channel consisting of parallel flat plates with periodic insertion of heat sources is low due to flow stagnation between consecutive heat sources [3]. The increase in the heat transfer in consecutive heat sources depends largely on the lateral walls cooling of the heated blocks where the flow is trapped. Young et al. [4] conducted a two-dimensional numerical parametric study in a channel containing multiple heated blocks. His study has involved obstacle height, and width, spacing, number of obstacles, obstacle thermal conductivity ratio, and heating method of obstacles over Reynolds number range of 200 to 2,000 based on hydraulic diameter.

McEntire et al. [5] investigated local forced convective heat transfer coefficient of an array of four discrete heat sources. Their investigation takes into account three different element heights and two different channel clearance heights with fixed stream-wise element spacing over Reynolds numbers range from 1,000 to 10,000. Results from this work suggest that the buoyancy factor is negligible.

Jubran et al. [6] experimentally explored the effect of the size of modules and missing modules on the performance of imitated electronic components within Reynolds number ranged from 1,690 to 2,625. They concluded that the rectangular modules tend to improve heat transfer by as much as forty percent over that of square modules and an improvement up to 37 % on the subsequent missing module.

Leung et al. [7] introduced an experimental work that included an electronic printed circuit board by examining periodic rectangular ribs in a channel flow. This research performed a parametric study on channel height, rib height, and rib width for both vertical and horizontal orientations of the channel over Reynolds number range from 510 to 2050. The study concluded that a choice of a flat rib with a larger top surface area is a more appropriate option since it enhances heat dissipation.

Meamer [8] performed a parametric study involving the effect of element height, width, spacing and heat flux distribution within 4,000 $\leq Re_H \leq$ 12,000. They found that Reynolds number has the most contribution to the heat removal in electronic packages. In the second rank comes the element width has an inverse effect on the heat transfer rates while increasing the spacing enhances the heat transfer.

Wang et al. [9] investigated the influence of flow rate and element height for a four elements array in a channel with uniform constant heat flux. The investigation of flush and protruding obstacles revealed that free convection plays an important role in the underlying physics when dealing with flush-mounted discrete heat sources, but it can be ignored in protruding cases when the Reynolds number exceeds 1500.

Abdulmajeed [10] investigated four geometric groove shapes: circular, rectangular, trapezoidal and triangular to perform the study, as well as two aspect ratios of groove-depth to tube diameter (e/D = 0.1 and 0.2) within a range of Reynolds number from 10,000 to 20,000. It was found that the grooved tube provides a considerable increase in heat transfer at about 64.4 % over the smooth tube. The problem of slow recirculating flow in grooved channels have addressed [11, 12].

Herman and Kang [13,14] identified six characteristic regions along the heat source. Regions (IV, V) on the upstream heat source and (IV, V, II) on the downstream one are characterized by low heat transfer surfaces; these regions are illustrated in Fig. 1.

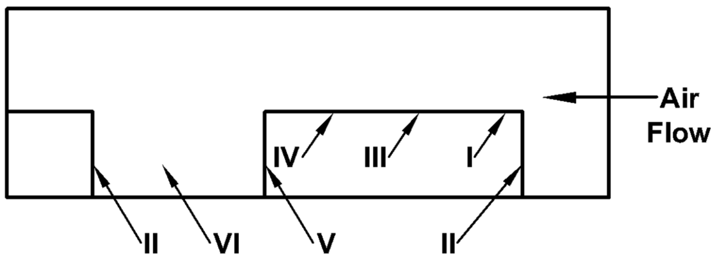

Fig.1. Sketch of region of interest.

Several researchers has revealed that heat transfer in grooved channels can be enhanced through improving lateral mixing by disrupting the shear layer separating the bulk flow and the recirculating flow [15-18]. Herman and Kang [15] were able to increase the heat transfer through the addition of cylinders and vanes by a factor of 1.2– 1.8 and 1.5 -3.5 within $200 \leq Re_L \leq 6500$, respectively. Herman and Kang [17] visualized unsteady temperature fields in the grooved channel with curved vanes using holographic interferometer in laminar flow. Heat transfer shows an increase by a factor of 1.5–3.5, when compared to the basic grooved while the pressure drop is 3–5 times higher than in the basic grooved channel.

Ko and Anand [19] investigated experimentally the module average heat transfer coefficients in uniformly heated rectangular channel with porous baffles mounted alternatively on the top and bottom of the walls. The heat transfer enhancement with porous baffles as high as 300% compared to heat transfer in straight channel with no baffles. Billen and Yapici [20] studied experimentally the enhancement of the heat transfer from a heated flat plate with rectangular blocks at different orientation angles. The maximum heat transfer rate is obtained at the orientation angle of 45°.

Anderson and Moffat [21] used curved vanes to improve the cooling of discrete electronic components through increased thermal mixing in the coolant flow. They found that their approach induces smaller pressure drop than conventional tabulators for a given decrease of the operating temperature. Fu and Tong [22] performed a numerical study on the influence of an oscillating cylinder located at the entrance to the horizontal channel with inserted periodical heated blocks. The results demonstrated that the rate of heat transfer increases surprisingly with oscillation of the cylinder in the region near the top of the block. The heat transfer increases 120% compared to the case when there is no cylinder in the horizontal channel. From the available literature, the enhancement of slow recirculating flow in stagnation zone between the heat sources is attractive where many studies at lower Reynolds number and small ratios of channel to heat source height were introduced.

The present work aims to investigate experimentally the effect of curved deflector radius and vertical and horizontal positions on both upstream and downstream heat sources. Reynolds number is varied from 5,223 to 11,338 at channel to heat source height ratio 0f 6.6. The measurements were utilized to introduce experimental correlation for the average Nusselt number of upstream and downstream heat sources as a function of investigated parameters.

EXPERIMENTAL SETUP

A schematic drawing of the experimental setup used is shown in Fig. 2. The test rig is composed basically from a wind tunnel operated in open suction mode. The flow system consists of air blower, flow orifice, transition duct, straightener, main duct including the test section, and bell-mouth. Airflow is drawn into the wind tunnel through a straightener to prevent the transmission of a swirl motion of the air stream from the fan back into the working section. AC motor of 1.5 hp is used to achieve inlet velocities range from 1.8 m/s up to 4 m/s. A horizontal duct of 200 mm width, 100 mm height and 2500 mm length. The test section composed of the two heat sources and curved deflector is located at a distance of **1175** mm from bell-mouth. Two pressure holes are located on each side of the test section to measure the pressure drop.

Heater Block Assembly

Two typical heat sources of 50 mm length and width with 15 mm height are mounted on a circuit board plate. The gap length between the heat sources is maintained at 50 mm in the stream wise direction. The heat source is hollowed and heated by a nickel-chromium wire with a resistance 256 Ω for each block. The nickel chromium wire is wrapped around an insulated tube with equal pitch and each heater is inserted inside the hollow block as shown in Fig. 3. Five Pre-calibrated thermocouples made of copper constantan wires are embedded in grooves through the internal surfaces of the heating element, one thermocouple on the top surface and four thermocouple on the side surfaces. Another thermocouple was inserted in wind tunnel intake to record the inlet fluid temperature. To minimize the heat losses, the lower side of the heating element is insulated where two thermocouples are embedded to estimate the heat loss. Fifteen channels data acquisition system is used to record the thermocouples readings. The input power to the heater is regulated with a 25 watt / 2 Amp DC power supply. A

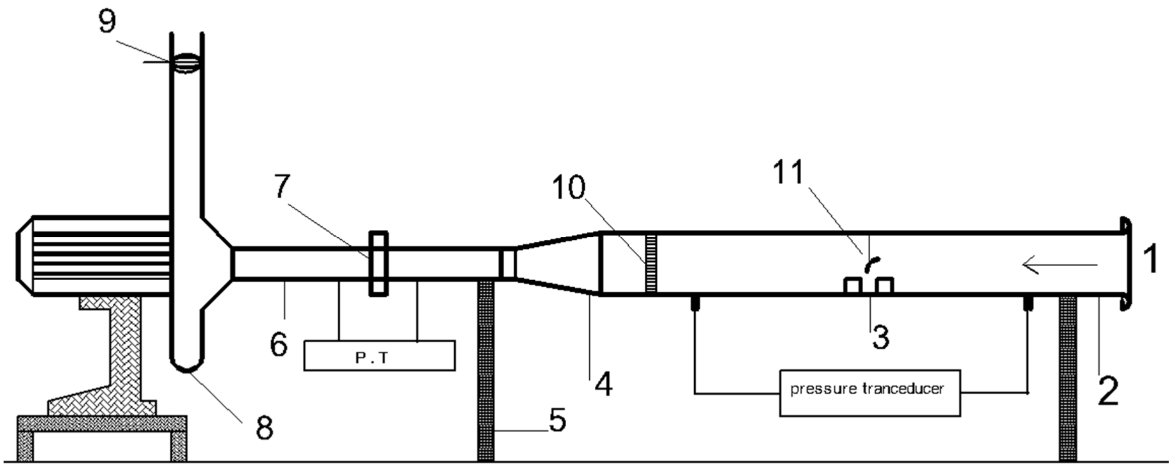

1- Bell mouth 2- Entrance Length 3- Test Section 4 -Transition Duct 5- Steel Stand 6–connecting pipe 3" 7- Orifice Meter 8- Air Blower 9- Discharge Gate 10-Straightener 11- Curved Defector

Fig. 2. Experimental Setup.

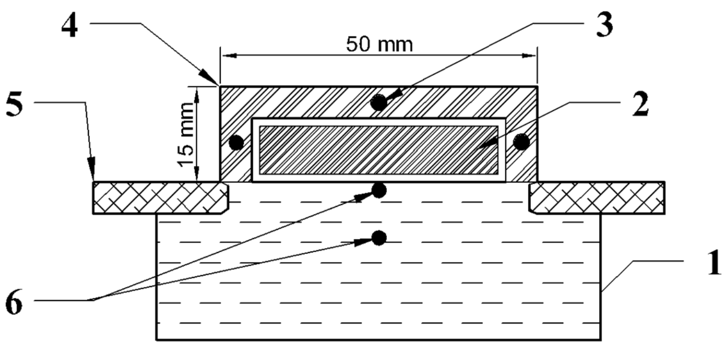

1- Asbestos insulation 2- Electric heater 3- Five thermocouples(one on top surface and 4 in vertical sides) 4-Brass heat source 5- base (circuit board) 6-Two thermocouples

Fig. 3. Details of the heat source.

digital differential manometer with accuracy 1 pa is used to measure the pressure drop across the test section and the orifice meter.

Deflector

Three curved deflector as a quarter of copper tube with radius 7.5, 14 and 17.5 mm (same width of 50 mm) are used to direct the flow toward the gap between the heat sources. The deflector is fixed to the top wall through an opening such that the horizontal and vertical distances can be varied (x=1, 10 and 20 mm, y=15, 20 and 25 mm) as shown in Fig. 4.

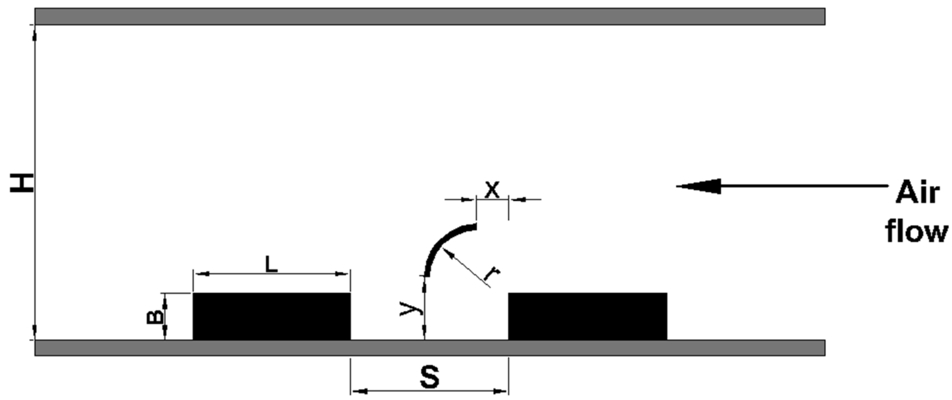

Fig.4. Sketch of the geometry under analysis.

EXPERIMENTAL PROCEDURES AND DATA REDUCTION

Before each data series, the deflector is installed at required position (R_x,R_y). The discharge gate at the blower outlet and supplied voltage to the heating element were turned on and adjusted for predetermined values. Once the heating element reaches steady state, the surface temperatures, inlet air temperature, pressure drop across the orifice meter and the test section and voltage drop of heater are recorded. A series of experiments were carried out for heat sources without deflector within the range of Reynolds number from 5223 to 11,338. Three different deflector dimensionless radius R_r=0.15, 0.28 and 0.35 were investigated at nine position of R_x and R_y (R_x=0.02, 0.2 and 0.4: R_y= 0.5, 0.4 and 0.3). The input electrical power to the heat sources is corrected for radiation and back conduction losses.

$$q_{net} = q_{in} - q_{rad} - q_{cond} \quad (1)$$

The input electrical power to the heater installed inside of the heat source (q_{in}) is calculated from q_{in}=V^2/R. The conduction loss is mainly from the lower side of the heat source through the insulation. The conduction and radiation losses in all experiments do not exceed 10% of the input electrical power. The applied heat flux (q''_{net}) on the internal surface of each heat source (A_s) is calculated from;

$$q''_{net} = \frac{q_{net}}{A_s} \qquad (W/m^2) \quad (2)$$

The results are presented in terms of the average convective heat transfer coefficient as,

$$h = \frac{q''_{net}}{T_m - T_a} \quad (3)$$

where, T_m is the average temperature for the heat source and T_a is the inlet fluid temperature at the inlet.

Average Nusselt number Nu along the surface of the heat source is expressed in the terms of heat transfer coefficient (h) , and the thermal conductivity of air (k) .

$$\mathrm{Nu} = \frac{\mathrm{h}*\mathrm{L}}{\mathrm{K}} \tag{4}$$

The friction factor is calculated from the recorded pressure drop across test section as;

$$f = \frac{\Delta P*\left(\frac{\mathrm{D_h}}{l}\right)}{\frac{1}{2}\rho \mathrm{U_{ave}}^2} \tag{5}$$

UNCERTAINTY ANALYSIS

The differential approximation presented by El-Shazly [23] was applied to determine the error in a result (F) which is a function of the independent parameters $\mathrm{x_1}$, $\mathrm{x_2}$,, $\mathrm{x_3}$,....., $\mathrm{x_n}$ as:

$$\mathrm{F} = F(\mathrm{x_1}, \mathrm{x_2}, \mathrm{x_3}, \dots\dots..\mathrm{x_4}) \tag{6}$$

The maximum absolute error in the result F can be written as,

$$|\Delta\mathrm{F}|_{\mathrm{max}} \approx \sum_{\mathrm{i=1}}^{\mathrm{n}} \frac{\partial \mathrm{F}}{\partial \mathrm{x_i}} \Delta \mathrm{x_{i,max}} \tag{7}$$

The overall uncertainty in the function F can be estimated from

$$|\partial\mathrm{F}|_{\mathrm{max}} \approx \frac{|\Delta\mathrm{F}|_{\mathrm{max}}}{\mathrm{F}} \approx \sum_{\mathrm{i=1}}^{\mathrm{n}} \frac{\partial \mathrm{F}/\partial \mathrm{x_i}}{\mathrm{Fx_i}} \Delta \mathrm{x_{i,max}} \tag{8}$$

The average Nusselt number is a function of element length, the fluid thermal conductivity and all parameters control the convective heat transfer coefficient. These parameters are the applied voltage, heater resistance, the heat transfer area, the average surface temperature and the fluid temperature. The overall uncertainty in the experimental data of the average Nusselt number is estimated using Eq. (8) as,

$$\frac{(\partial \mathrm{Nu_L})_{\mathrm{max}}}{\mathrm{Nu_L}} = 2*\frac{|\Delta\mathrm{V}|_{\mathrm{max}}}{\mathrm{V}} + \frac{|\Delta\mathrm{R}|_{\mathrm{max}}}{\mathrm{R}} + \frac{|\Delta\mathrm{A_s}|_{\mathrm{max}}}{\mathrm{A_s}} + \frac{|\Delta\mathrm{T_m}|_{\mathrm{max}}}{(\mathrm{T_m}-\mathrm{T_a})} + \frac{|\Delta\mathrm{T_a}|_{\mathrm{max}}}{(\mathrm{T_m}-\mathrm{T_a})} \tag{9}$$

Similarly, the uncertainty in Reynolds number was obtained using the same equation as a function of the relative measured error in heat source length and the average velocity that depends on the pressure drop across orifice meter,

$$\frac{(\partial \mathrm{Re_L})_{\mathrm{max}}}{\mathrm{Re_L}} = 0.5*\frac{|\Delta\mathrm{P_{Or}}|_{\mathrm{max}}}{\mathrm{P_{Or}}} + \frac{|\Delta\mathrm{L}|_{\mathrm{max}}}{\mathrm{L}} \tag{10}$$

The maximum uncertainty in Reynolds number is 6.2% at Re_L = 5223 and the corresponding uncertainty in Nu_L = 9.1%. These values are based on the assumption of negligible uncertainty in the relevant fluid properties.

RESULTS AND DISCUSSION

To confirm of the validity of the present experimental measurements, the average Nusselt number for a single heat source for different Reynolds number are compared with Jubran and Al-Salaymeh [24] as shown in Fig. 5. Also the obtained results for friction factor in turbulent flow are compared with the correlation of Petukhov [25]

$$f = (0.79 \mathrm{Ln Re_{Dh}} - 1.64)^{-2} \quad (11)$$

The maximum error between the present measurements and the correlated values of Petukhov [25] is 7.1% as shown in Fig.6. This good agreement reveals the accuracy of the experimental setup and used measurement technique.

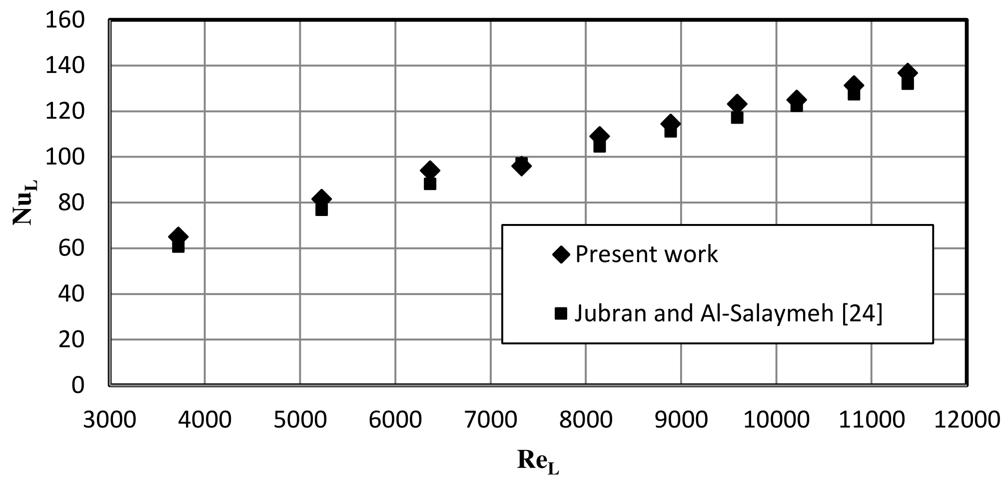

Fig. 5. Validation of Nusselt number for single heat source.

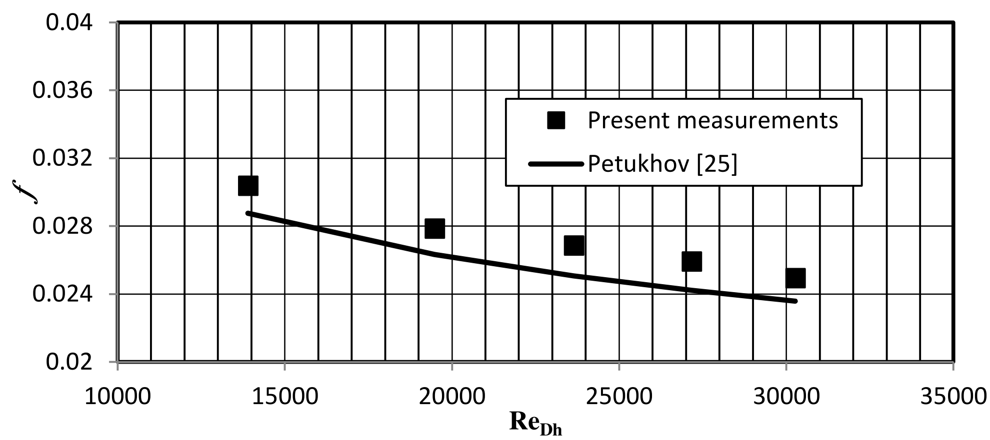

Fig. 6. Validation of Friction factor for smooth channel.

Heat Transfer Results

The heat transfer performance for upstream and downstream heat sources was compared to the case with no deflector. Firstly, a series of experiments were performed without curved deflector for the basic module of two heat sources in turbulent flow region, corresponding to mean flow velocity from U_{ave} = 1.89 to 4 m/sec that representative for flow velocity in electronic cooling application. Then number of series of experiments were carried out to investigate the effect of deflector dimensionless radius(R_r), dimensionless horizontal and vertical positions (R_x,R_y). Three different radius deflector R_r=0.15, 0.28, and 0.35 were studied. The dimensionless horizontal and vertical distances are changed such that R_x=0.02, 0.2 and 0.4 and R_y= 0.5, 0.4 and 0.3. The mass flow rate is changed and adjusted for each position such that 5223 ≤ Re_L ≤ 11,338.

Effect of horizontal position

Figures 7 and 8 show the effect of the horizontal distance R_X on heat transfer rate in term of average Nusselt number for upstream and downstream heat sources, respectively. In General, it can be seen that the presence of the deflector along the downstream edge of the upstream heat source enhances the heat transfer rate from the module when compared with the basic module without deflector. This can be attributed to the changes in the flow structure within gab between the heat sources from recirculating flow in basic module to jet-like flow formed between the deflector and the heated blocks. By this phenomenon, the curved deflector enhances the heat transfer rate from vertical surface V and region IV (shown in Fig. 1). It is clear from Fig.7 that placing the deflector near to the upstream heat source R_x=0.02, enhances the heat transfer rate from upstream heat source. This is attributed to the acceleration of the flow trapped by the deflector and discharged into the trailing edge of the upstream heat source (regions III, IV and V). At $Re_L = 11338$, an enhancement in the average Nusselt number of 19% is obtained for the upstream heat source at R_r=0.35 and R_y=0.3.

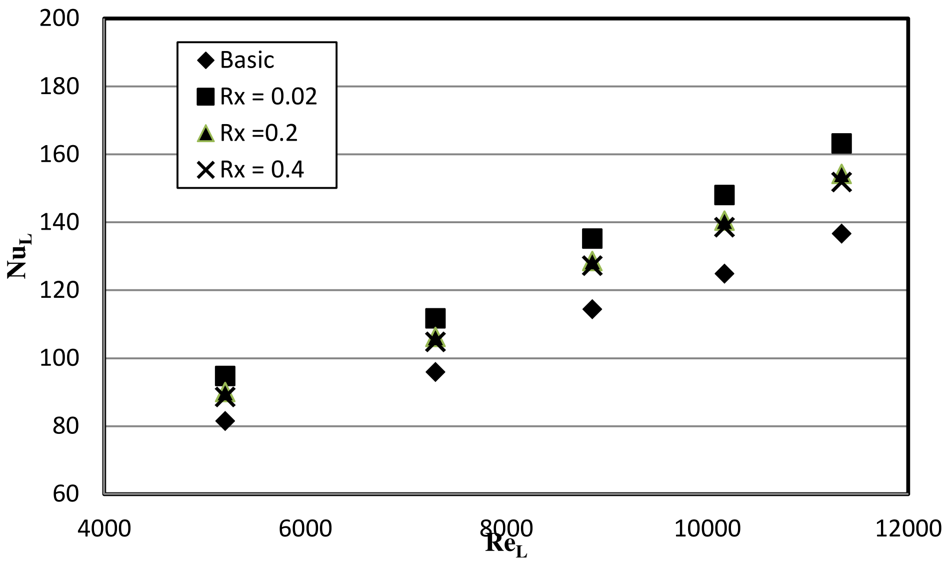

Fig. 7. Nusselt number versus Reynolds number for upstream heat source, ($\boldsymbol{R_r}$ = 0.35 and $\boldsymbol{R_y}$ =0.3: Rx refers to $\boldsymbol{R_x}$).

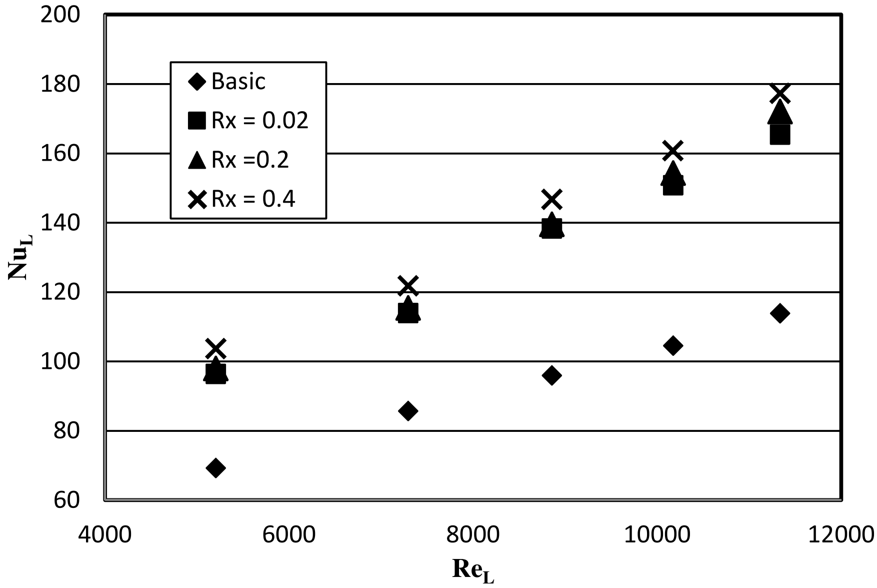

Fig. 8. Nusselt number Versus Reynolds number for downstream heat source, (R_r = 0.35 and R_y = 0.3).

A noticeable effect of the deflector on the heat transfer rate from the downstream heat source was obtained as shown in Fig. 8. It is clear that increasing in the horizontal distance enhances the average heat transfer coefficient of downstream heat source. This is returned to moving the deflector towards region II of the downstream block allows the flow passes below the deflector not only breaks the recirculation zone but generate jet-like flow on regions II and I of the downstream heat source. From Figs. 7 and 8, the obtained downstream Nusselt number exceeds the obtained values of upstream heat source without deflector. At $Re_L = 11338$, an enhancement of 56% in average Nusselt Number is obtained for $R_x = 0.4$ at R_r=0.35 and R_y=0.3 as illustrated Tables 1 and 2 .

Effect of deflector vertical position ($\mathbf{R}_y$)

The influence of the vertical position $\mathrm{R_y}$ on heat transfer rate from the two heat sources are shown in Figs. 9 and 10. It is noticed that the presence of the deflector near the recirculation zone at lower $\mathrm{R_y}$ enhances the heat transfer rate from both heat sources when compared with the basic module. This is mainly returned to the thermal mixing in the recirculation zone due to the directed flow by the deflector. Also, this can be attributed to the compression of the thermal boundary layer in the regions IV, V and VI on the upstream block and flow accelerating in regions I, III and IV on the downstream heat source. From Table 1, the maximum enhancement is 19% at $\mathrm{R_x} = 0.02$ for the upstream heat source and 56% for the downstream one at $\mathrm{R_x} = 0.4$ for $\mathrm{R_y} = 0.3$ $\mathrm{R_r} = 0.35$ and $\mathrm{Re_L} = 11338$.

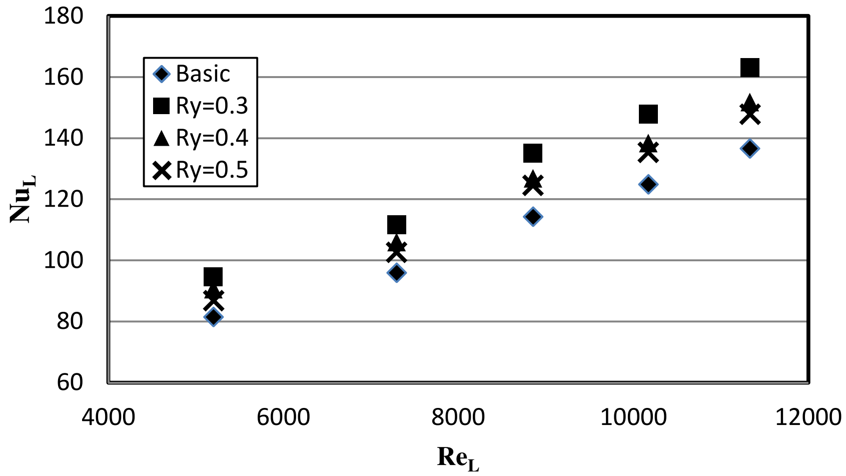

Fig. 9. Average Nusselt number Versus Reynolds number for upstream heat source,($\mathrm{R_r} = 0.35$ and $\mathrm{R_x} = 0.02$).

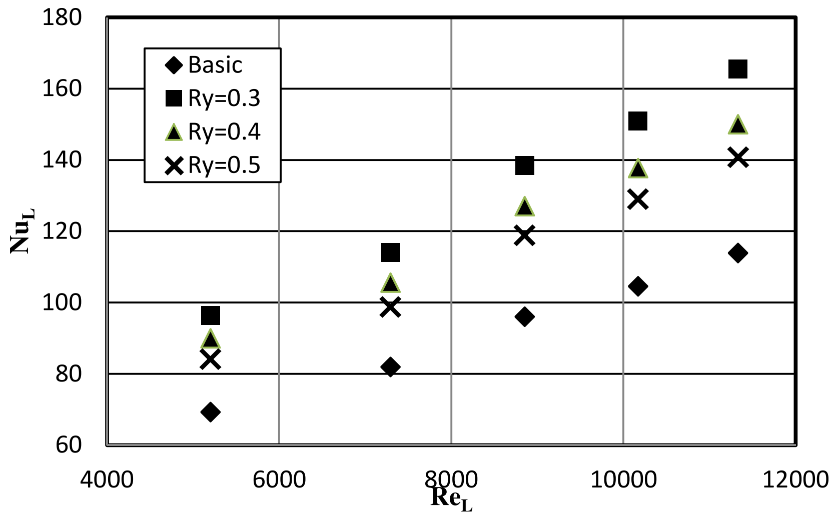

Fig. 10. Average Nusselt number versus Reynolds number for Downstream heat source, $R_r = 0.35$ and $R_x = 0.02$).

Effect of deflector radius ($\mathbf{R_r}$)

Figures 11 and 12 illustrate the effect of the of the curved deflector radius R_r on heat transfer rate. The dimensionless deflector radius is changed 0.15 to 0.35 for the ranges 0.02 $\leq R_x \leq$ 0.4 and 0.5 $\leq R_y \leq$0.3. It is clear that the increase in deflector radius enhances heat transfer rate from both heat sources. This is returned to the curved deflector of larger size enhances the jet flow towards the recirculation zone and as explained by Ortiz and Hernande [26]. With moving the deflector toward the downstream heat source, the enhancement in the average Nusselt number for the downstream exceeds the upstream heat source. This can be returned to compression of the thermal boundary layer and the thermal mixing due to the jet flow. At $\mathrm{Re_L} = 11338$, the enhancement in the average Nusselt number for the downstream heat source is of 56% at $\mathrm{R_x}$ = 0.4 and $\mathrm{R_y}$=0.3 as illustrated in Table 1.

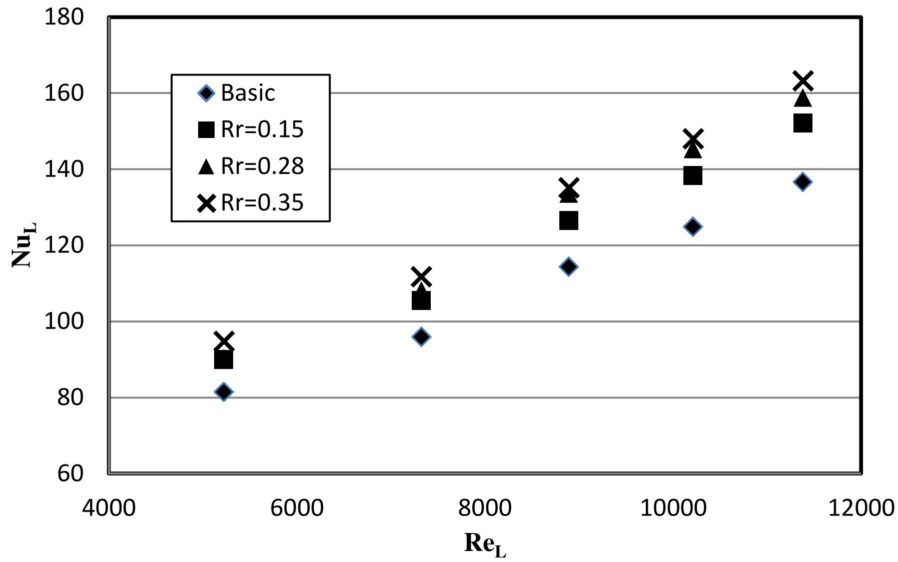

Fig. 11. Average Nusselt number Versus Reynolds number for upstream heat source,($\boldsymbol{R_x}$ = 0.02 and $\boldsymbol{R_y}$ =0.3)

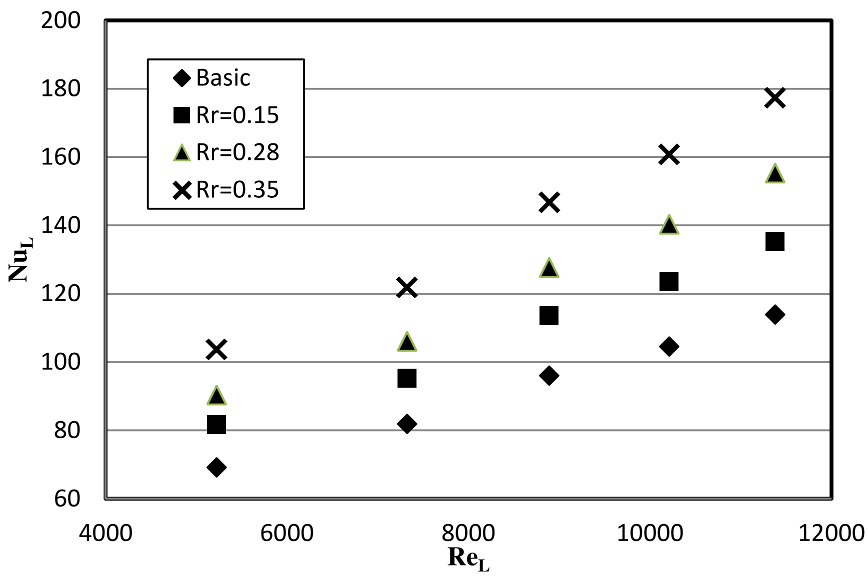

Fig. 12. Average Nusselt number Versus Reynolds number for downstream heat source, ($\boldsymbol{R_x}$ = 0.4 and $\boldsymbol{R_y}$ = 0.3).

Performance Criterion

Tables 1 and 2 present the ratio of measured average Nusselt number with deflector $\mathrm{Nu_{def}}$ relative to the corresonding values for basic module without deflector $\mathrm{Nu_{bas}}$ for each heat source separately for range $5223 \leq \mathrm{Re_L} \leq 11338$, $0.02 \leq \mathrm{R_x} \leq 0.4$, $0.3 \leq \mathrm{R_y} \leq 0.5$ and $0.15 \leq \mathrm{R_r} \leq 0.35$. It is clear that the best enhancement for the upstream heat source occurs at R_x=0.02, as we gain **16% to 19%** enhancement for the largest deflector of $\mathrm{R_r}$ = 0.35 at $\mathrm{R_y}$=0.3. This enhancement decreases at R_x=0.4 and $\mathrm{R_y}$=0.5 for all deflector radius used, and the lowest values occurs for the smallest deflector of

Table 1. Nu_{def}/Nu_{bas} for upstream heat source.

Rr	Re	Ry= 0.5			Ry= 0.4			Ry= 0.3		
		Rx=0.02	Rx=0.2	Rx=0.4	Rx=0.02	Rx=0.2	Rx=0.4	Rx=0.02	Rx=0.2	Rx=0.4
0.15	5223	1.03	1.02	1.02	1.06	1.04	1.03	1.10	1.07	1.06
	7323	1.03	1.01	1.01	1.06	1.04	1.03	1.10	1.06	1.05
	8890	1.05	1.02	1.02	1.06	1.05	1.04	1.11	1.07	1.06
	10211	1.05	1.02	1.01	1.06	1.05	1.04	1.11	1.07	1.06
	11338	1.05	1.03	1.01	1.07	1.05	1.05	1.11	1.08	1.06
	Re	Rx=0.02	Rx=0.2	Rx=0.4	Rx=0.02	Rx=0.2	Rx=0.4	Rx=0.02	Rx=0.2	Rx=0.4
0.28	5223	1.06	1.04	1.03	1.09	1.06	1.05	1.11	1.08	1.06
	7323	1.06	1.04	1.03	1.09	1.06	1.06	1.13	1.09	1.07
	8890	1.07	1.04	1.04	1.10	1.06	1.08	1.17	1.11	1.10
	10211	1.06	1.04	1.03	1.10	1.06	1.07	1.16	1.11	1.10
	11338	1.05	1.04	1.02	1.10	1.06	1.07	1.16	1.11	1.11
	Re	Rx=0.02	Rx=0.2	Rx=0.4	Rx=0.02	Rx=0.2	Rx=0.4	Rx=0.02	Rx=0.2	Rx=0.4
0.35	5223	1.06	1.05	1.04	1.11	1.08	1.07	1.16	1.10	1.09
	7323	1.07	1.04	1.04	1.11	1.07	1.07	1.16	1.11	1.09
	8890	1.09	1.05	1.04	1.11	1.07	1.08	1.18	1.12	1.11
	10211	1.08	1.04	1.04	1.11	1.08	1.07	1.18	1.12	1.11
	11338	1.08	1.04	1.04	1.11	1.08	1.07	1.19	1.13	1.11

Table 2. Nu_{def}/Nu_{bas} for downstream heat source.

Rr	Re	Ry= 0.5			Ry= 0.4			Ry= 0.3		
		Rx=0.02	Rx=0.2	Rx=0.4	Rx=0.02	Rx=0.2	Rx=0.4	Rx=0.02	Rx=0.2	Rx=0.4
0.15	5223	1.06	1.08	1.13	1.8	1.11	1.15	1.10	1.15	1.18
	7323	1.06	1.08	1.12	1.08	1.10	1.14	1.09	1.13	1.16
	8890	1.06	1.11	1.15	1.09	1.11	1.16	1.10	1.15	1.18
	10211	1.07	1.11	1.14	1.09	1.12	1.16	1.10	1.15	1.18
	11338	1.07	1.1	1.14	1.09	1.14	1.17	1.10	1.16	1.19
	Re	Rx=0.02	Rx=0.2	Rx=0.4	Rx=0.02	Rx=0.2	Rx=0.4	Rx=0.02	Rx=0.2	Rx=0.4
0.28	5223	1.21	1.23	1.24	1.24	1.26	1.29	1.25	1.27	1.30
	7323	1.20	1.22	1.24	1.22	1.25	1.28	1.24	1.27	1.29
	8890	1.22	1.26	1.28	1.25	1.30	1.31	1.26	1.31	1.33
	10211	1.22	1.25	1.27	1.24	1.30	1.31	1.26	1.32	1.34
	11338	1.22	1.26	1.27	1.24	1.30	1.32	1.26	1.34	1.36
	Re	Rx=0.02	Rx=0.2	Rx=0.4	Rx=0.02	Rx=0.2	Rx=0.4	Rx=0.02	Rx=0.2	Rx=0.4
0.35	5223	1.21	1.23	1.26	1.30	1.32	1.40	1.39	1.42	1.50
	7323	1.21	1.23	1.26	1.29	1.31	1.37	1.39	1.41	1.49
	8890	1.24	1.26	1.29	1.32	1.34	1.39	1.44	1.45	1.53
	10211	1.23	1.26	1.30	1.32	1.35	1.40	1.44	1.48	1.54
	11338	1.24	1.27	1.31	1.32	1.37	1.41	1.45	1.51	1.56

radius $\mathrm{R_r}$ =0.15 where it does not exceed 1%. Table 2 shows that best enhancement for the downstream heat source occurs at R_x=0.4, an enhancement of 18% to 56% for the largest deflector of $\mathrm{R_r}$ = 0.35 at $\mathrm{R_y}$=0.3. This enhancement decreases at R_x=0.02 and $\mathrm{R_y}$=0.5 for all deflector radius used, and the lowest values occurs for the smallest deflector of radius $\mathrm{R_r}$ = 0.15 where it does not exceed 6%.

Empirical Correlations

In order to describe the influence of deflector radius and position on the performance of the module, empirical correlations have developed. These correlation predict the average Nusselt number, Nu as a function of the investigated parameters: $\mathrm{Re_L}$,$\mathrm{R_r}$,$\mathrm{R_x}$and $\mathrm{R_y}$. The data is correlated and presented. It can be expressed as:

a) Upstream heat source

$$Nu_{def} = 0.177\, Re_L{}^{0.7096}\, R_r{}^{0.0435}\, R_x{}^{-0.0131}\, R_y{}^{-0.1271} \tag{12}$$

b) Downstream heat source

$$Nu_{def}=0.2499\, Re_L{}^{0.7005}\, R_r{}^{0.2255} R_x{}^{0.01835}\, R_y{}^{-0.1711} \tag{13}$$

Equation (11) and (12) are valid for $5223 \leq \mathrm{Re}_L \leq 11338$, $0.02 \leq \mathrm{R_x} \leq 0.4$, $0.3 \leq \mathrm{R_y} \leq 0.5$ and $0.15 \leq \mathrm{R_r} \leq 0.35$ with maximum deviation 6% and 9% the upstream and downstream heat sources, respectively.

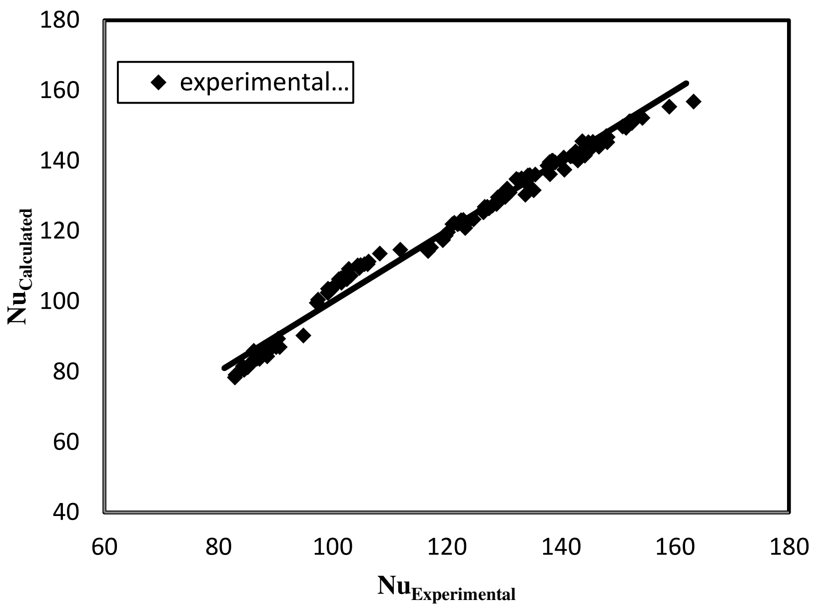

Fig. 13. Correlated versus experimental data for upstream heat source (Equation 12).

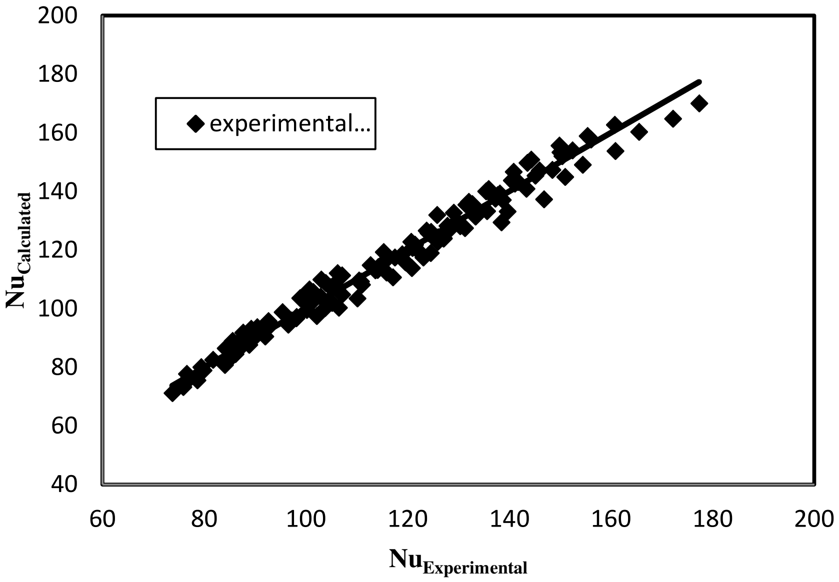

Fig. 14. Correlated versus experimental data for downstream heat source (Equation 13).

FRICTION FACTOR

Figure 15 shows the friction factor versus Reynolds number for the module of two heat sources with different deflector radius compared to the basic module without deflector. The friction factor sustains an asymptotic value $\mathrm{Re_L} \geq 10000$. The friction factor (f) reaches about (1.8 to 3.9) times the friction factor of the basic module for R_r varies from 0.15 to 0.35. The vertical and horizontal positions have a negligible effect on friction factor within the investigated ranges.

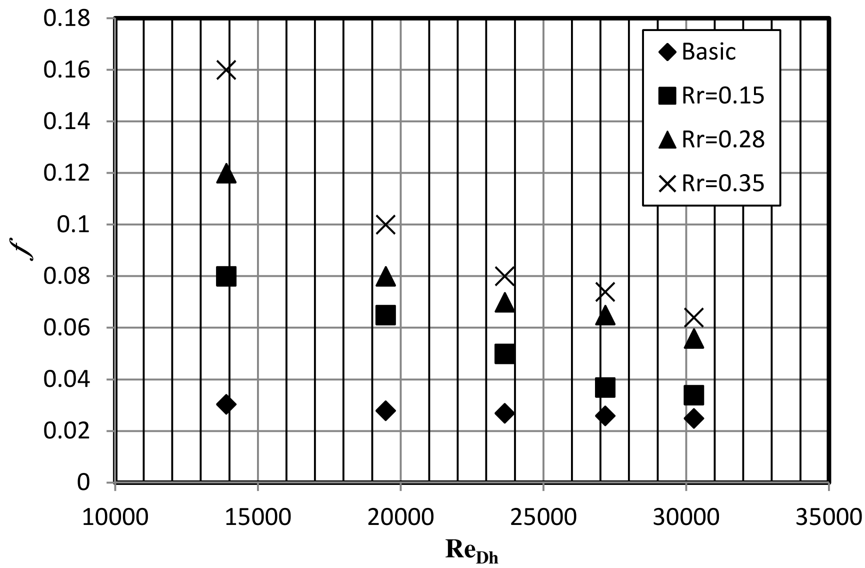

Fig. 15. Friction factor Vs Reynolds number.

CONCLUSIONS

The experimental results reveal that using the deflector is advantageous in order to provide higher thermal performance especially at high Reynolds number. Fluid mixing in the recirculation zone between the heat sources is largely responsible for enhanced rates of heat transfer of the heat sources. However, applying larger deflectors causes a larger pressure gradient, generating unfortunately a larger friction loss. It is recommended to install the deflectors in a vertical position equals to the heat source for all deflector radii and horizontal positions. The results show that horizontal distance R_x has a contrast effect on the thermal performance of two heat sources. The best enhancement for the upstream heat source is obtained at R_x=0.02 where an enhancement in the average Nusselt number of 16% to 19% for the largest deflector of $\mathrm{R_r}$ = 0.35 at $\mathrm{R_y}$=0.3. However, an enhancement of 18% to 56% is obtained for the downstream heat source at $R_x = 0.4$ and $\mathrm{R_r}$ = 0.35. The present measurements indicates that pressure drop depends mainly on deflector radius while a negligible effect for the defector position is noticed. The friction factor (f) reaches 1.8 to 3.9 times the friction factor of the basic module when R_r varies from 0.15 to 0.35 within the investigated ranges.

REFERENCES

[1] P. Rodgers,V. Eveloy, M.G. Pecht, Limits of air-cooling: status and challenges: 21st IEEE Semi-Therm Symposium, 2005.

[2] R. Schmidt, Challenges in electronic cooling-opportunities for enhanced thermal management techniques-microprocessor liquid cooled mini-channel heat sink, Heat Transf. Eng. 25(3), (2004), 3–12.

[3] C. Herman, E. Kang, Comparative evaluation of three heat transfer enhancement strategies in a grooved channel, Heat Mass Transfer 37 (2001) 563–575.

[4] T.J. Young, k. Vafai, Convective flow and heat transfer in a channel containing multiple heated obstacles, Int. J. Heat Mass Transfer 41(1998) 3279–3298.

[5] A.B. McEntire, B.W Webb, Local forced convective heat transfer from protruding and flush-mounted two-dimensional discrete heat sources, Int. J. Heat Mass Transfer 33(7) (1990) 1521–1533.

[6] B.A. Jubran, S.A. Swiety, M.A. Hamdan, Convective heat transfer and pressure drop characteristics of various array configurations to simulate the cooling of electronic modules. Int. J. Heat Mass Transfer. 39(16) (1996) 3519–3529.

[7] C.W. Leung, H.J . Kang, Convective heat transfer from simulated air-cooled printed circuit board on horizontal or vertical orientation. Int. Comm. Heat Mass Transfer 25(1) (1998) 67–80.

[8] E. Meamer, Forced Convection Heat Transfer in Two-Dimensional Ribbed Channels with Varying Heat Flux Profiles Using ANSYS' Software and Modeling. Arab J. Sci. Eng. 39 (2014)2157–2164.

[9] Y. Wang, K. Vafai, Heat transfer and pressure loss characterization in a channel with discrete flush and protruding heat sources. Exp. Heat Transfer 12(1999) 1–16.

[10] A.R. Abdulmajeed T.A. Yaser, J.S. Amer, Groove geometry effects on turbulent heat transfer and fluid flow, Heat Mass Transfer 49 (2013)185–195.

[11] C.H. Amon, B.B. Mikic, Numerical prediction of convective heat transfer in self-sustained oscillatory flows, J. Thermophys. Heat Transfer 4 (2) (1990) 239–246.

[12] B. Farhanieh, C. Herman, B. Sunden, Numerical and experimental analysis of laminar fluid flow and forced convection heat transfer in a grooved duct, Int. J. Heat Mass Transfer 36 (6) (1993) 1609–1617.

[13] C. Herman, E. Kang M. Wetzel, Expanding the applications of holographic interferometry to the quantitative Visualization of complex, oscillatory thermofluid processes, Exp. Fluids 24 (1998) 431-446.

[14] C. Herman, E. Kang, Experimental visualization of temperature fields and study of heat transfer enhancement in oscillatory flow in a grooved channel, Heat mass transfer 37(2001) 88-99.

[15] C. Herman, E. Kang, Comparative evaluation of three heat transfer enhancement strategies in a grooved channel, Heat Mass Transfer 37 (2001) 563–575.

[16] C. Herman, Experimental visualization of temperature fields and study of heat transfer enhancement in oscillatory flow in a grooved channel, Heat Mass Transfer 37 (2001) 87–99.

[17] C. Herman, E. Kang, Heat transfer enhancement in a grooved channel with curved vanes, Int. J. Heat Mass Transfer 45 (18) (2002) 3741–3757.

[18] C. Herman, E. Kang, An experimental study of convective heat transfer enhancement in a grooved channel using cylindrical eddy promoters, J. Enhanc. Heat Transfer 8 (2002) 1–19.

[19] Kang-Hoon Ko, N.K. Anand, Use of porous baffles to enhance heat transfer in a rectangular channel, Int. J. Heat Mass Transfer 46 (22) (2003) 4191–4199.

[20] Kang-Hoon Ko, N.K. Anand, Use of porous baffles to enhance heat transfer in a rectangular channel, Int. J. Heat Mass Transfer 46 (22) (2003) 4191–4199.

[21] A.M. Anderson, R.J. Moffat, Direct air cooling of electronic components: reducing component temperatures by controlled thermal mixing, J. Heat Transfer 113 (1991) 56–62.

[22] F. Wu-Shung , T. Bao-Hong , Numerical investigation of heat transfer characteristics of the heated blocks in the channel with a transversely oscillating cylinder, Int. J. Heat Mass Transfer 47 (2) (2004) 341–351.

[23] K.M. El-Shazly, Effect of Darcian and non-Darcian natural convection on the effective thermal conductivity of a porous medium, Ph.D. Thesis, Faculty of Engineering, Cairo University, 1991.

[24] B. A. Jubran and A. S. Al-Salaymeh, Heat transfer enhancement in electronic module using ribs and "film-cooling-like" techniques, Int. J. Heat and Fluid Flow 17(1996) 148-154.

[25] B.S. Petukhov, Heat transfer in turbulent pipe flow with variable physical properties. N.Y.: Academic Press, 1970.

[26] L. Luviano-Ortiz a, A. Hernandez-Guerrero, C. Rubio-Arana, R. Romero-Mendez, Heat transfer enhancement in a horizontal channel by the addition of curved deflectors, Int. J. of Heat and Mass Transfer 51 (2008) 3972–3984.